https://doi.org/10.15407/ujpe68.5.349

I.A. LYASHENKO,[1,2] V.L. POPOV[1]

[1] Technische Universität Berlin, Institut für Mechanik,
FG Systemdynamik und Reibungsphysik
(Sekr. C8–4, Raum M 122, Strasse des 17. Juni 135, 10623 Berlin, Germany;
e-mails: i.liashenko@tu-berlin.de, v.popov@tu-berlin.de)
[2] Sumy State University
(2, Rimskogo-Korsakova Str., Sumy 40007, Ukraine)

CORROSION EFFECT ON THE ADHESIVE STRENGTH OF A CONTACT BETWEEN A HARD INDENTER AND A SOFT ELASTOMER: AN EXPERIMENTAL STUDY

The influence of the duration of a contact between a steel indenter susceptible to the corrosion and a water-containing gelatin-based elastomer on the contact adhesive strength has been studied. It is shown that the growth in the contact duration leads to the substantial contact strengthening. As a result, the contact becomes so strong that the pulling of the indenter out of the elastomer causes the destruction of the elastomer surface.

Keywords: corrosion, elastomer, adhesive strength, indentation, quasi-static contact.

1. Introduction

A domain in mechanics dealing with the study of contact processes has been actively developed in recent decades. Although the most famous classic work in this direction [1] was published more than 140 years ago, a strong impetus to the development of the mechanics of contact interactions has been gained just recently. This occurred due to the emergence of fundamentally new methods of numerical analysis and the growth in the power of modern computing facilities, as well as the improvement of experimental research methods. Modern universal numerical methods used for simulating the contact processes include the finite-element method [2], the boundary-element method [3, 4], the method of movable cellular automata [5], and the molecular dynamics methods [6].

Note that the boundary-element method was modified in [7, 8] to calculate contact problems making allowance for the adhesion. Despite that the adhesive contact has been studied for several decades (starting from fundamental works [9–11]), there still remain a lot of unsolved issues in this area, which induce a lively discussion in leading scientific groups. For example, not fully understood are the mechanisms of adhesive interaction between rough surfaces [12–14], the influence of the adhesion on the friction force at the motion in tangential contacts [15, 16], and so forth.

In the previous work [8], an experimental setup was described and was used to perform a number of experiments aimed at studying the detachment processes of flat surfaces of various geometric shapes from the elastomer surface with high adhesion. As the elastomer, the solidified aqueous solution of gelatin was applied.

Citation: Lyashenko I.A., Popov V.L. Corrosion effect on the adhesive strength of a contact between a hard indenter and a soft elastomer: An experimental study. *Ukr. J. Phys.* **68**, No. 5, 349 (2023). https://doi.org/10.15407/ujpe68.5.349.
Цитування: Ляшенко Я.О., Попов В.Л. Вплив корозійних процесів на адгезійну міцність контакту між жорстким індентором і м'яким еластомером: експеримент. *Укр. фіз. журн.* **68**, №5, 348 (2023).

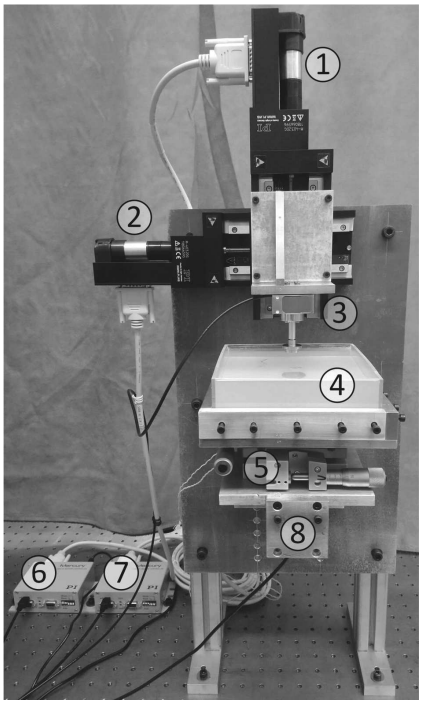

Fig. 1. Appearance of experimental setup (see also [14, 17]). The labeled elements are described in the text

In what follows, we call the experimental gelatin specimen the elastomer, because it has typical elastomer properties, in particular, a capability to sustain large deformations in the practically complete absence of volume compression). In work [8], the detachment of indenters with flat bases from gelatin was considered. In this paper, we describe experiments with the indentation of spherical and cylindrical indenters into gelatin, as well as the influence of the contact duration on the adhesion force. The main distinction of the proposed research from the earlier studies consists in that the indenter contacting with gelatin (which is mostly composed of water) was made of a corroding steel. In this case, corrosion processes considerably affect the adhesive properties of the contact. The main goal of the proposed work is to study the influence of the corrosion on the adhesion strength of the contact.

2. Experimental Technique

In Fig. 1, a photo of the device developed to study adhesion processes is exhibited. Here, labels *1* and *2* denote the directional movement drives PI M-403.2DG (they were controlled by PI C-863 controllers *6* and *7*). Label *3* marks a triaxial force sensor ME K3D40. A four-channel amplifier GSV-1A4 SubD37/2 was used to amplify the electrical signal given by the sensor, and a 16-bit ADC NI USB-6211 to transmit the amplified signal to a computer. A steel indenter was attached to the force sensor; in the experiment, it was immersed into elastomer *4* (the solidified aqueous solution of gelatin). The elastomer surface could be fixed at various angles in two directions with the help of tilting mechanism *5*. The evolution of the contact area was monitored with the help of a video camera mounted at position *8*. The described installation allowed independent movements of the indenter to be performed in both the normal and tangential directions, which made it possible to carry out comprehensive studies of adhesive contacts (a more detailed description of the equipment capabilities was given in the recent work [17]). In the presented work, we describe experiments aimed at studying normal contacts.

Similarly to works [8, 18], jelly as a medium with adhesive properties was used in all experiments described here. The jelly mass was obtained by solidifying ordinary nutrient gelatin fabricated by the Dr. Oeteker company (Germany). The solution was prepared by diluting 4 gelatin bags of 9 g each in 1 liter of water. At this concentration, the produced jelly remained in a stable solid state at room temperature (about 24 °C). The jelly was poured into a rectangular plexiglass container $150\times150\times40$ mm^3 in dimensions (40 mm was the layer thickness). The resulting volume of the solution was 900 ml.

After the gelatin had solidified, a steel indenter whose surface had been preliminarily polished to a mirror state was brought into contact with it. Then the indentation process took place followed by the indenter detachment.

3. Corrosion Effect on Adhesive Strength

For the initial test, a cylindrical indenter with the base radius $a = 5$ mm and made of a stainless steel was used. The corresponding experimental results are shown in Fig. 2. The indenter was brought into contact with the elastomer surface. Then it was indented to the depth $d \approx 2$ mm at the constant velocity $v = 0.01$ mm/s. Afterward, it was moved in the opposite direction until the contact completely disappeared. It follows from Fig. 2 that, within the interval

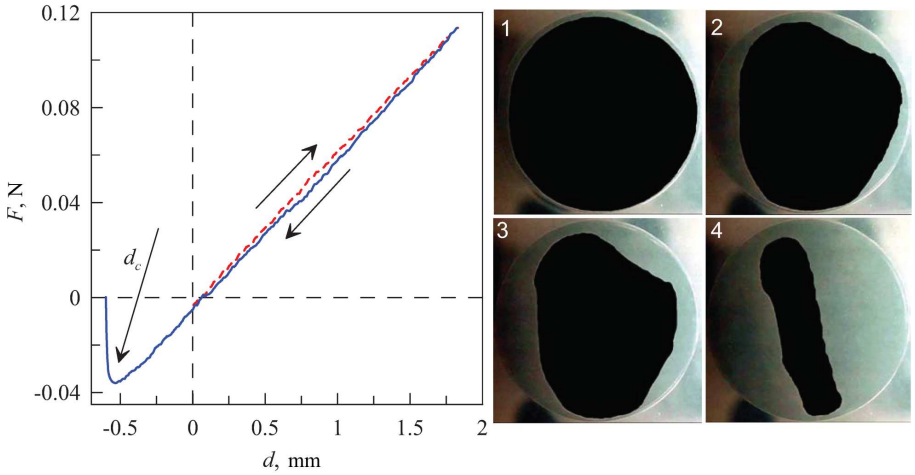

Fig. 2. Dependences of the normal force F on the indentation depth d for the indentation of a cylindrical stainless steel indenter with the radius $a = 5$ mm into elastomer. Photos *1–4* on the right demonstrate the contact area at the stage of its destruction; the available contact is colored black

of positive indentation depths, the dependence $F(d)$ is close to linear.

Using the definition of the incremental contact stiffness $k = \mathrm{d}F/\mathrm{d}(d)$, we can find the contact stiffness value $k \approx 64$ N/m. On the other hand, in the case where a rigid indenter is in contact with an elastic half-space, the stiffness k can be determined using the formula [19]

$$k = 2E^* a, \tag{1}$$

where E^* is the reduced elastic modulus of the elastomer. The elastomer that was used in our experiments can be considered with a sufficient accuracy as occupying the half-space, because its thickness $h = 40$ mm substantially exceeded both the contact radius $a = 5$ mm and the indentation depth $d < 2$ mm. Since the values of k and a are known from the experiment, expression (1) leads to the value of the reduced elastic modulus of the elastomer $E^* = 6.4$ kPa. The critical value of the indentation depth (d_c, this is the distance between the surfaces of the indenter and the elastomer at which the contact completely collapses) is determined by the known formula [19]

$$d_c = -\sqrt{\frac{2\pi a \gamma_{12}}{E^*}}, \tag{2}$$

where γ_{12} is the specific adhesion work. From whence, it is easy to find this parameter.

The experimental determination of γ_{12} is much more difficult than the experimental determination of the elastic modulus, because it is almost impossible to set the elastomer and indenter surfaces perfectly in parallel to each other. Moreover, those surfaces always contain inhomogeneities. Therefore, in practice, the contact destruction happens somewhat earlier than the theory predicts.

Figure 2 also demonstrates the photos of the contact area between the cylindrical indenter and the elastomer in the course of contact destruction. Photo *1* shows that the detachment does not begin simultaneously over the whole contact area. During the detachment process, the indicated non-uniformity substantially increases (photos *2–4*). However, the detachment is observed over the entire contact area rather than in a certain selected corner. This fact testifies that the experimental surfaces were oriented in parallel to each other with rather high accuracy. According to the dependence $F(d)$ in Fig. 2, the critical value of the indentation depth equals $d_c \approx -0.56$ mm. Formula (2) and the determined quantities bring about the value $\gamma_{12} \approx 0.064$ J/m^2.

Figure 3 demonstrates the experimental results for the indentation of a steel sphere into the same elastomer (see Fig. 2). However, now (Fig. 3), the indenter was made of a corrodible steel. Figure 3 shows the results of three consecutive experiments (three indentation/detachment cycles), and the correspond-

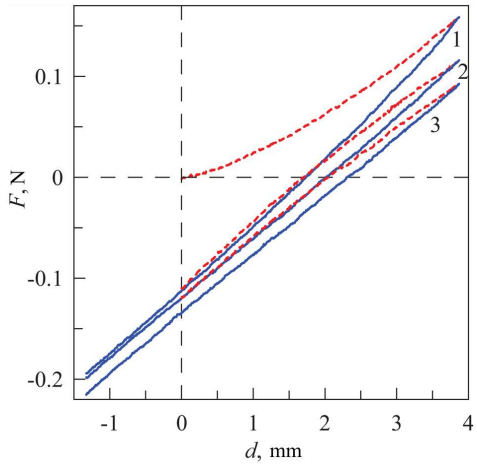

Fig. 3. Dependence of the normal force F on the indentation depth d for the indentation of a spherical indenter with the radius $R = 11$ mm and made of a corroding steel into elastomer

ing dependences are marked by labels *1–3*. The value of the specific adhesion work can differ from that found above, when analyzing Fig. 2, because γ_{12} depends on the physical properties of both contacting bodies. However, as a rule, γ_{12} differs insignificantly among various steel grades. Nevertheless, if the indenter is made of a corrodible steel, γ_{12} changes considerably with the growth of the contact duration time. In our experiment, the indentation was performed at a low velocity of the indenter motion, $v = 1$ μm/s. This value was chosen to provide quasistatic contact conditions. Then, during one indentation cycle, the indenter was in contact with the elastomer (whose water content exceeded 95%) for more than 2.5 h.

The dashed curves in Fig. 3 show those sections of the dependences that were obtained at the indentation stage, whereas the solid sections of the curves correspond to the detachment stage. Three consecutive indentation cycles were performed, which are marked by labels *1* to *3*. In the first cycle, the normal force F first increases to some maximum value. When the indentation depth becomes equal to $d \approx 4$ mm, the indenter starts to move in the reverse direction, but its displacement is no longer described by the initial dependence $F(d)$. It follows from the figure that $F(d)$ demonstrates some linear dependence at the detachment stage. This behavior means that the contact radius and the contact stiffness remain constant. The origin of this behavior consists in the following. During the indenter–elastomer interaction, the indenter surface within the contact area with the elastomer has enough time to be oxidized (corroded), so that the indenter becomes strongly "stuck" to the elastomer. In a certain sense, this process is similar to how contacting metal parts can stick to each other after their mutual oxidation and the appearance of corrosion products in the contact zone. The presence of corrosion products increases the specific adhesion work γ_{12} many times over, so the contact area practically does not change further, when the indentation depth d changes within the given limits.

The preservation of the constant contact area when changing the direction of the indenter motion was also observed in the contact of a metal indenter with rubber [20], i.e., in the absence of corrosion processes. However, in this case, when the indenter moves in the reverse direction, there is always a moment, when the contact radius begins to decrease due to the destruction of adhesive bonds and without the destruction of the elastomer. In this paper, we describe a situation where the contact can be strengthened so much that the indenter detachment takes place with the mandatory elastomer destruction in the bulk.

In the experiment (its results are illustrated in Fig. 3), after the indenter was lifted to some fixed maximum height $d < 0$ mm above the elastomer surface, it was quickly returned to the level $d = 0$ mm at the velocity $v = 0.1$ mm/s. Then, after a one-minute pause, the indentation process was repeated. In all experimental dependences, there are no dashed sections at negative indentation depths, because the values of the acting forces F and the corresponding indenter shifts d were not saved, when the indenter moved rapidly.

From Fig. 3, it follows that, after the first indentation cycle, the other cycles are characterized by almost linear dependences $F(d)$, which correspond to an almost constant contact area. However, those curves deviate from the straight-line behavior at large indentation depths. Such a behavior testifies that the contact configuration does change at large d. The corresponding changes result, in particular, from the thinning of the jelly layer due to water evaporation from its surface (this effect is described below in detail). Each subsequent indentation cycle increases the magnitudes of the force F in the interval of negative d-values (when the indenter rises above the elastomer

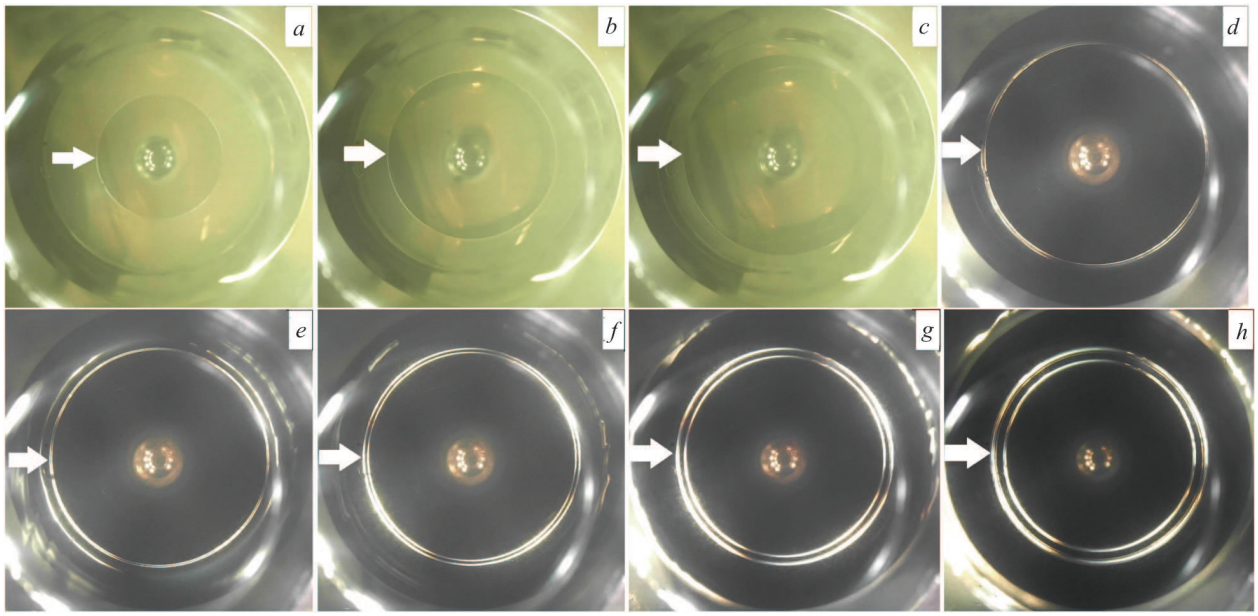

Fig. 4. Appearance of a contact between a spherical indenter and elastomer (jelly) in the course of indentation and detachment at various indentation depths: $d = 1$ mm (indentation) (a), $d = 2$ mm (indentation) (b), $d = 3$ mm (indentation) (c), $d = 3$ mm (detachment) (d), $d = 2$ mm (detachment) (e), $d = 1$ mm (detachment) (f), $d = 0$ mm (detachment) (g), $d = -1$ mm (detachment) (h)

surface), which is also a result of the elastomer thickness reduction.

Figure 4 demonstrates the photos of the contact configuration in the case of indentation with a sphere with the radius $R = 11$ mm (see Fig. 3). Since a mirror-polished indenter was used, its surface reflected the elements of the environment. In particular, at the center of the photos, one can see the images of the LED elements, which were located near the base of a video camera. Despite those features, the contact boundary is clearly visible (shown by a white arrow in all photos).

The figure caption quotes the values of the indentation depth d at which the corresponding photos were taken. Photos a–c correspond to the indentation stage during which the indentation depth and the contact area increased monotonically. Photo d corresponds to the same d-value as in photo c ($d = 3$ mm). In photos e–h, the contact radius practically does not change, although they correspond to the detachment stage. The origin of the contact radius stability at the stage, when the indenter was pulled out of the elastomer, is a substantial contact strengthening, which occurred at the indentation stage owing to the indenter surface corrosion.

An interesting feature here is that two rings are observed in photos e–h at the contact boundary. This optical effect is associated with the appearance of an adhesive neck in the contact area. The diameter of the neck at its center is smaller than at the point of the indenter–elastomer contact. Such a neck is visually displayed in the form of two distinct light rings, because the contact is photographed from below (see Fig. 1). In photo e, the image of the adhesive neck (two very close rings) is shown by an arrow. The larger (open) ring may probably be a remnant of the destroyed contact boundary, because the gelatin material is partially torn out of the elastomer layer, when the indenter is pulled out.

Figure 5, a contains a photo of the contact area at the beginning of indentation (at $d = 0$ mm) in the second indentation cycle (dependence *2* in Fig. 3). From this figure, it follows that the contact configuration remained practically the same as in panels f–h in Fig. 4. This fact means that, during the second indentation cycle, the contact configuration and size remain unchanged in a wide interval of indentation depths d, although the contact was absolutely absent at $d = 0$ mm in the first cycle. A closed circle with the largest radius in Fig. 5, a corresponds to the physical

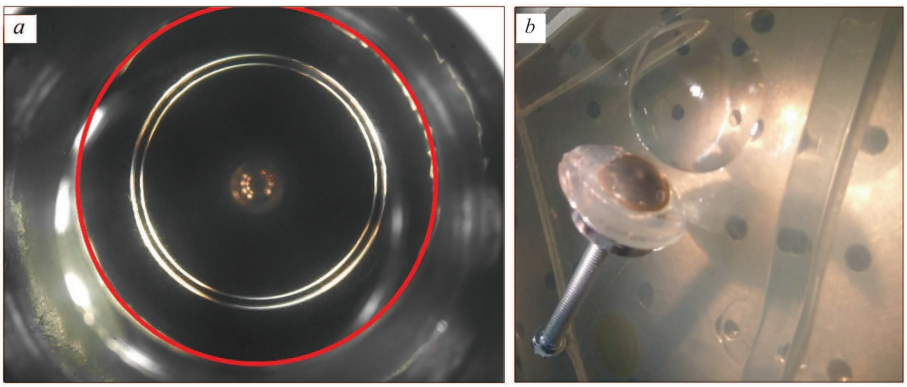

Fig. 5. Photo of the contact area between a spherical indenter and elastomer (jelly) at the beginning of the second indentation cycle (see curve *2* in Fig. 3) (*a*). Photo of the indenter on the elastomer (jelly) surface after the contact collapsed (*b*)

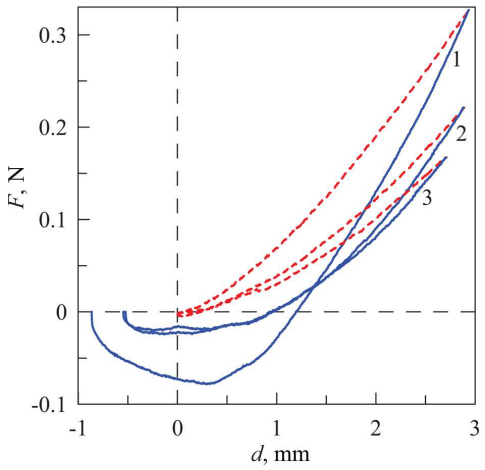

Fig. 6. Dependences of the normal force F on the indentation depth d for the indentation of a spherical indenter with the radius $R = 22$ mm and made of a corrodible steel into elastomer

boundaries of the steel indenter, which coincide with similar boundaries in Fig. 4. The diameter of this circle equals 2 cm.

Figure 5, *b* exhibits the indenter after its detachment from the elastomer (jelly) surface. To perform such an action, a much greater force than the maximum force in Fig. 3 had to be applied. When pulling out the indenter from the elastomer, a significant part of the latter was extracted leaving a deep spherical dimple, which can also be observed in Fig. 5, *b*. The indenter, which was mirror-polished before the experiment, lost its mirror-like properties in the contact area due to the corrosion, and its surface acquired a characteristic yellow shade.

The results of the next series of experiments with an indenter with the larger radius $R = 22$ mm are shown in Fig. 6. Three indentation cycles were also performed here. However, in contrast to the case described above, now, the total destruction of the adhesive contact took place in each indentation cycle, when the indenter was detached from the jelly. Furthermore, the adhesive strength of the contact (the minimum external force that had to be applied in order to destroy the contact) was much higher for the first indentation cycle (curve *1*) than for the subsequent cycles. This is a result of corrosion processes. In all three indentation cycles, when the indenter was being detached from the elastomer, the contact area decreased monotonically to zero. But the partial destruction of the elastomer (jelly) surface already occurred in the first cycle, and some quantity of elastomer remained on the indenter surface. Therefore, in the course of the two next indentation cycles, the indenter surface had areas, where the indenter did not create direct contacts with the elastomer, but where the elastomer was in contact with itself, and such a contact had a weaker adhesive strength. The normal force F corresponding to the maximum of the indentation depth d substantially decreased in every subsequent indentation cycle. This effect was mainly induced by a reduction in the elastomer (the aqueous solution of gelatin) thickness owing to the evaporation of moisture from the elastomer surface and, partially, by the destruction of the elastomer surface in each subsequent indentation cycle.

The photo of the indenter with the radius $R = 22$ mm after its detachment from the elastomer

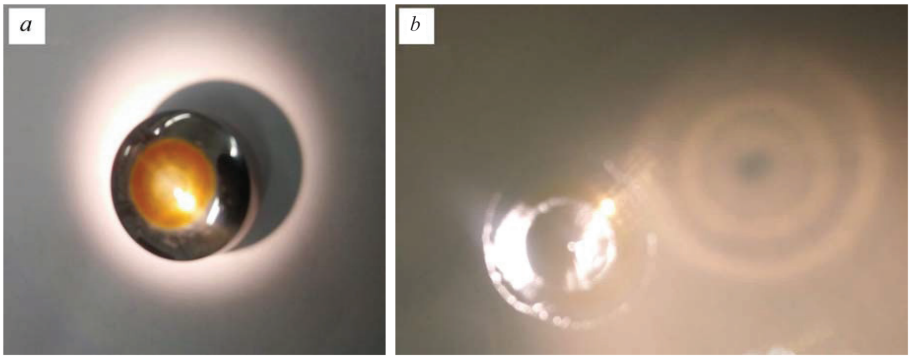

Fig. 7. Photos of an indenter with the radius $R = 22$ mm (a) and the elastomer surface after the experiment (b)

is shown in Fig. 7, a. In this case, it was not necessary to apply an additional force to destroy the contact, because the destruction occurred at the depths falling within the interval of indentation depths used in the experiment (see Fig. 6). In Fig. 7, a, one can distinctly see the traces of corrosion at the indenter center, which changed the color of indenter surface in the contact area. In addition, there are elastomer particles on the indenter surface, but their volume is much smaller than that observed in Fig. 5, b.

The degree of the contact area destruction is well illustrated in Fig. 7, b, where the photo of the elastomer surface after three complete indentation cycles is shown. The enlarged image of the contact area, which was formed by a light stream passing through the elastomer surface is seen in the upper right corner of the photo. This image clearly demonstrates separate circles with different radii, and their presence testifies to the heterogeneous character of the destruction process.

4. Influence of Contact Duration

The experiments described above showed that, in the presence of corrosion processes in the contact zone, the duration of the contact substantially affects its adhesive strength. For a detailed elucidation of the character of this influence, an additional series of experiments was carried out, in which a cylindrical indenter with the diameter $D = 10$ mm was immersed into the elastomer (jelly) at the velocity $v = 5$ μm/s to the depth $d = 1.5$ mm. Then the indenter was left in this position for a fixed time interval T and afterward raised to the distance $d = -6$ mm above the jelly surface (the values $d < 0$ corresponded to the indenter positions above the elastomer surface) at the same velocity of 5 μm/s.

In this experimental series, an newly-prepared elastomer was used. Despite that it was prepared in a similar way, its elastic characteristics might differ from those described above, so a series of additional experiments were performed to determine them. The obtained results are shown in Fig. 8.

Figure 8, a demonstrates the dependences of the normal force F on the indentation depth d obtained in the experiment, where the influence of the indenter stop time T on the adhesive strength was studied. The numbers near the curves indicate the values of the time interval T (in minutes) during which the indenter remained at rest in contact with the elastomer at the maximum indentation depth. First, the elastomer (jelly) was cooled down in a refrigerator; then, it was warmed up at room temperature for several hours; afterward, the indentation experiment was carried out. The first experiment was executed for the indenter stop time $T = 120$ min. The corresponding load curve $F(d)$ at the indentation stage (the first quarter of the coordinate dependence, the upper dashed curve) has a different slope in comparison with those of other curves, which, in this case, corresponds to a larger value of the elastic modulus of elastomer. This occurred, because the elastomer had not enough time to warm up to room temperature before the first experiment started. However, at the indenter detachment stage, the slopes of all dependences $F(d)$ are approximately identical, and it is the detachment stage at which the contact adhesive strength was studied in this work.

All the dependences shown in Fig. 8, a demonstrate a reduction of the elastic force, when the indenter is

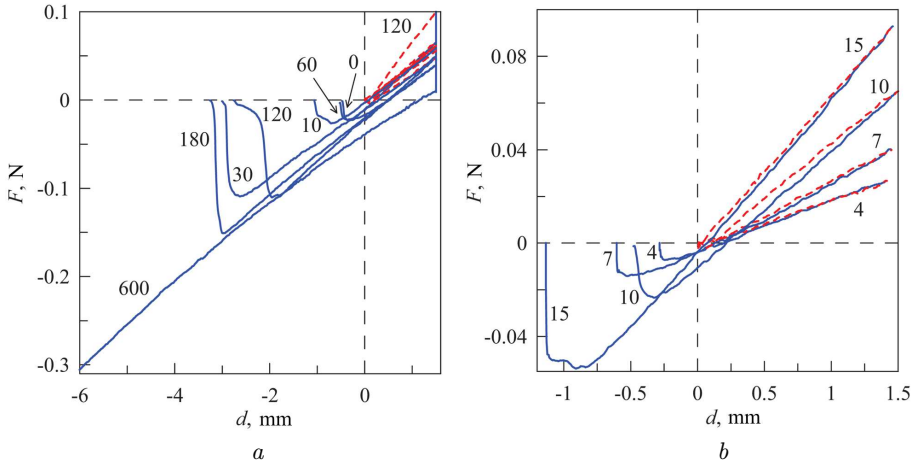

Fig. 8. Dependences of the normal force F on the indentation depth d for the indentation of a cylindrical steel indenter with the diameter $D = 10$ mm into elastomer (jelly)(a). The numbers near the curves indicate the indenter stop time (in minutes) at the maximum indentation depth $d_{\max} = 1.5$ mm. Experimental results for the indentation of cylindrical indenters with various diameters (indicated in millimeters near the corresponding curves) made of a stainless steel (b). The dependences for the indenter with the diameter $D = 10$ mm in panels (a) and (b) are identical: this indenter was made of a corrodible steel

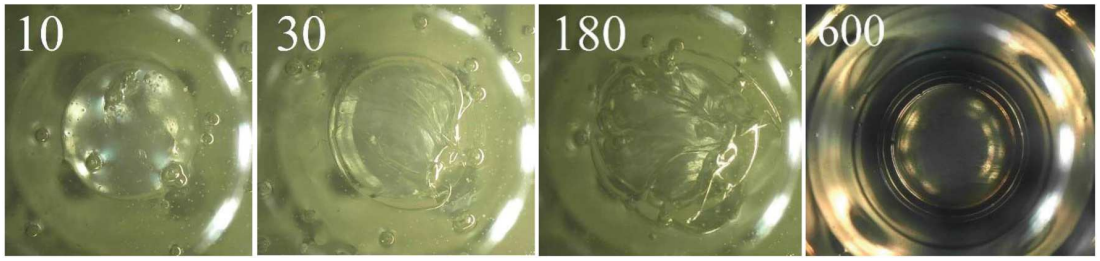

Fig. 9. Photos of the contact areas after the experiments, the results of which are shown in Fig. 8, a. The panels are labeled with the values of indenter stop time T (in minutes)

at rest. Therefore, the curve $F(d)$ corresponding to the detachment stage passes always lower than the analogous dependence for the load stage. This effect is especially noticeable for $T = 120$ min and $T = 600$ min. In the case $T = 120$ min, we associate it with the fact that the elastomer continued to heat up to room temperature during the first experiment. So, its elasticity decreased. At the same time, the force reduction in the experiment with $T = 600$ min is a result of the moisture evaporation from the elastomer (jelly) surface during the stop time interval, so that the elastomer became thinner.

In the experiment with the contact time $T = 600$ min, the indenter became "stuck" so strongly to the jelly due to corrosion processes that the complete destruction of the contact could be attained, only if some part of the elastomer surface was torn out of the total elastomer mass (see Fig. 5, b). Therefore, in this case, the complete contact took place even at the force $F = -0.3$ N (Fig. 8, a). At the same time, in the absence of a corrosion and for an indenter with the diameter $D = 10$ mm, the contact already collapsed at the force $F = -0.023$ N, which follows from Fig. 8, b (curve *10*).

In Fig. 8, a, the contact area did not collapse after the indenter was detached only in the cases $T = 0$ and 60 min. In other cases, the contact area became destroyed, and elastomer particles were present on the indenter. Due to the presence of chemical inhomogeneities and mechanical irregularities at the indenter surface, corrosion processes taking place there during the indentation process run unevenly [21]. If the indenter is held in contact for not a very long time (see, e.g., the curve for $T = 30$ min), the adhesive bonds that are strong enough for the elastomer to be destroyed, when the indenter is detached, are formed

only in some places. As a result, the indenter tears out the elastomer material from those surface places, where the bonds are most strengthened. Accordingly, both the absolute values of the critical force and the indentation depth at which the contact destruction occurs at the detachment stage increase. If the contact exists long enough (see the case $T = 600$ min), all areas have enough time to strengthen and the contact becomes stronger than the molecular bonds in the elastomer over the whole contact area. To destroy such a contact, it is necessary to apply a considerably larger force in comparison with the case of reverse destruction of adhesive bonds. All those factors bring us to the situation shown in Fig. 5, *b*.

In Fig. 9, the photos of the elastomer surface after the contact destruction are shown for those experimental values of the indenter stop time T that correspond to the dependences $F(d)$ in Fig. 8, *a*. As follows from Fig. 9, there is no damage in the case $T = 10$ min. At the same time, concentric circles are observed in the case $T = 600$ min. This result corresponds to a complete "sticking" of the indenter to the elastomer, and it is similar to that shown in Fig. 4 (panels *f*–*h*) and in Fig. 5, *a*. In Fig. 9 ($T = 10$, 30, and 180 min), the inhomogeneities described above are observed on the jelly surface in the form of open air bubbles, which afterward transform into craters that intensively evaporate moisture, which results in the degradation of the elastomer (jelly) surface [1].

Let us return to Fig. 8, *b*, which depicts the dependences $F(d)$ describing the indentation of cylinders with various diameters D (the specific D-values in millimeters are indicated near the corresponding curves). Using the measurement results, as well as formulas (1) and (2), we calculate the elastic and adhesive parameters of the elastomer. We obtained the following values for various indenters: $E^* \approx 5.3$ kPa and $\gamma_{12} \approx 0.026$ J/m^2 for $D = 4.0$ mm, $E^* \approx 4.2$ kPa and $\gamma_{12} \approx 0.048$ J/m^2 for $D = 7.0$ mm, $E^* \approx 5$ kPa and $\gamma_{12} \approx 0.026$ J/m^2 for $D = 10$ mm, and $E^* \approx$ ≈ 4.4 kPa and $\gamma_{12} \approx 0.059$ J/m^2 for $D = 15$ mm. As one can see, the elastomer parameters are somewhat different in different experiments, which confirms the temporal instability of gelatin parameters. For the elastomer specimen corresponding to Fig. 2, *a*, the parameters calculated in a similar way had close values: $E^* \approx 6.4$ kPa and $\gamma_{12} \approx 0.064$ J/m^2.

In the series of experiments, the results of which are shown in Fig. 8, the same elastomer specimen was used. However, as was mentioned above, the elastomer parameters change in time, which complicates the comparative analysis of the results obtained in different experiments. Therefore, an additional series of experiments were performed, in which seven identical specimens of jelly elastomers were prepared and stored at a temperature of 7 °C. The mass of each jelly object did not exceed 30 g, so it could be quickly heated up to room temperature. After a specimen was destroyed during the experiment, it was replaced by another one previously heated up to room temperature. In this series of experiments, the indenter was first plunged into the elastomer to the depth $d = 1.5$ mm and then lifted to the distance $d = -5$ mm. The corresponding results are shown in Fig. 10.

In Fig. 10, *a*, curves *1* show the dependence $F(d)$ obtained for the indenter stop time $T = 600$ min. The dashed part of the dependence corresponds to the indentation stage, and the solid part to the detachment stage. It follows from the figure that, during the time interval when the indenter remained static, the normal force F vanished and even changed its sign. A similar albeit less pronounced effect is observed in Fig. 8. It is a result of the intense moisture evaporation from the elastomer (aqueous jelly) surface into the environment, due to which the elastomer thickness decreases in time.

In order to make the presentation of experimental results convenient, let us exclude the effect of elastomer thinning from the dependences. At the load stage, the dependence $F(d)$ shown in Fig. 10, *a* corresponds to the contact stiffness $k \approx 28$ N/m. The corresponding maximum elastic force at the indentation depth $d = 1.5$ mm equals $F_1 \approx 0.0384$ N. Then the indenter is at rest for the time interval T. At the moment, when the indenter starts to move upward,

[1] This is a disadvantage of using gelatin as an elastomer in adhesion experiments, because its elastic properties change in time due to the moisture evaporation, so that the gelatin surface quickly degrades. When analyzing the experimental results, the indicated features giving rise to a lower reproducibility of experiments have to be taken into account. A good alternative is the application of the transparent grades of rubber [14, 15, 20], whose elastic and adhesive properties are much more stable over time. However, rubber of this type is not suitable as an elastomer for achieving the purpose of this work, i.e., to study the effect of the corrosion, when a steel indenter is in contact with water.

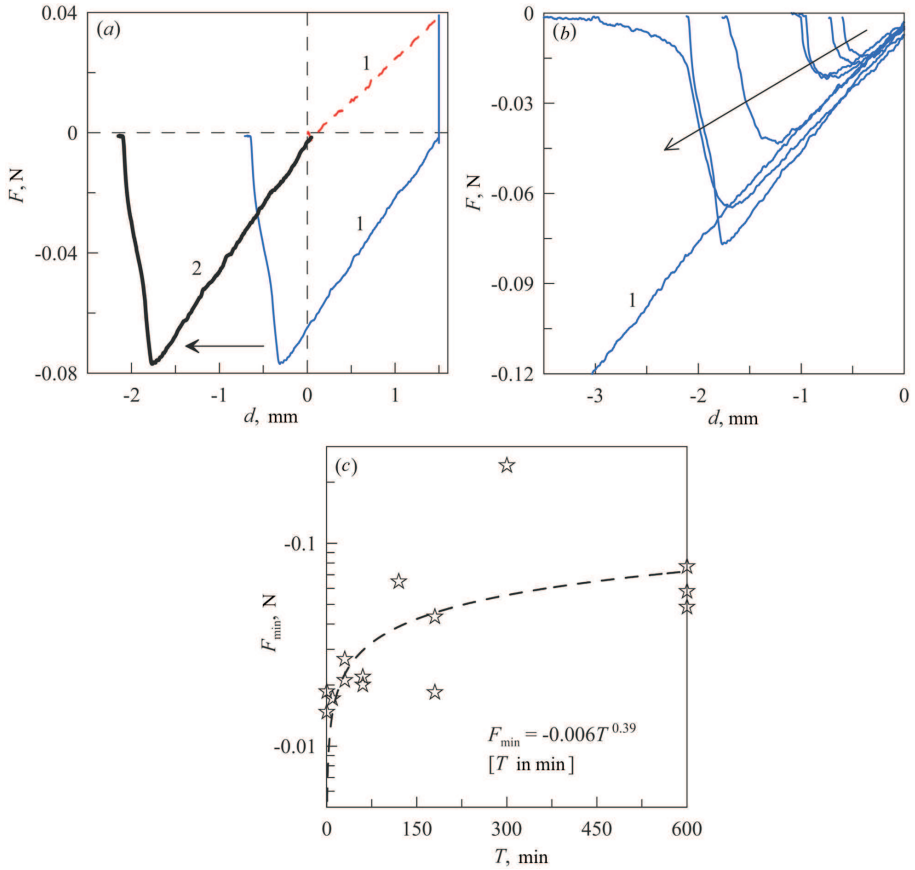

Fig. 10. Experimental dependence $F(d)$ obtained for the indenter stop time in contact $T = 600$ min (curve *1*; the dashed section corresponds to the indentation stage, and the solid one to the detachment stage) and the detachment section recalculated taking the reduction of the jelly thickness into account (curve *2*) (*a*); *b* – $F(d)$ dependences corresponding to the indenter detachment stage for various indenter stop times $T = 0$, 10, 60, 30, 180, 600, and 120 min (in the direction indicated by the arrow. Curve *1* corresponds to the stop time $T = 300$ min. *c* – the values of the minimum normal force $F_{\min}$ reached at the indenter detachment stage for various indenter stop times T (symbols; the values were obtained from the results partially shown in Fig. 10, *b*) and their approximation with power-law dependence (3)

the elastic force equals $F_2 \approx -0.0016$ N. The force difference is $\Delta F = F_1 - F_2 = 0.04$ N. Knowing the contact stiffness k, we calculate the variation of the elastomer thickness: $\Delta l = \Delta F/k \approx 1.43$ mm. Hence, during the time interval T, a layer of water whose thickness was approximately equal to the indentation depth was evaporated. The dependence $F(d)$ has to be left-shifted by the calculated Δl-value, which corresponds to the detachment of the indenter. This procedure is equivalent to the shift of lower curve *1* in Fig. 10, *a* to the left in such a way that it would touch the load curve (the dashed curve), because, in the case of cylindrical indenter, the indentation and detachment stages have to be described by the same dependence $F(d)$, if the elastomer thickness is constant. The dependence $F(d)$ recalculated in this way, which would correspond to the situation where the elastomer thickness does not change, is shown by curve *2* in Fig. 10, *a*.

The above-described parallel shift of the dependences $F(d)$ does not change the values of the normal force F. Therefore, it does not affect the value of the contact adhesive strength and is performed solely for the convenience of presentation of the experimental dependences in the same figure.

The shifted dependences obtained for various values of the indenter stop time T are shown in Fig. 10, *b*. The figure testifies that, on average, the

contact strengthens in time due to the corrosion. However, the experimental results do not demonstrate a monotonic increase of the contact adhesive strength as the time T grows. In particular, for $T = 300$ min (curve *1*), the contact does not collapse for the selected interval of indentation depths, but its destruction does take place at $T = 600$ min. This is so, because the time $T = 300$ min is long enough for the corrosion processes to occur over the whole contact area. The strength of adhesive bonds (taking the chemical corrosion processes into account) becomes much higher than that of cohesive bonds in gelatin. In both considered cases ($T = 600$ and 300 min), the indenter tears off some quantity of the elastomer from the surface, when the contact collapses, i.e., the contact area becomes destroyed. The contact strength can increase further. However, after the whole indenter surface has corroded rather strongly, and the adhesive bonds between the indenter and the elastomer have become stronger than the bonds between the molecules in the elastomer, the further enhancement of the contact strength does not affect the critical force at which the destruction occurs.

The critical force is affected by many other factors: the smoothness of the elastomer (jelly) surface, the parallelism of the elastomer and indenter surfaces, chemical and mechanical inhomogeneities, and others. It is the influence of those factors that leads to the non-monotonic character of the critical force dependence on the time T, which is shown in Fig. 10, *c*. The figure cumulates the results of several experiments that were performed with the same indenter stop time T. One can see that the experimental critical forces can be different for the same T-value. However, on average, the experimental results testify to the enhancement of the contact strength with the growth of the time T. The dashed curve in Fig. 10, *c* demonstrates the least-squares approximation of the experimental results by the power function

$$F_{\min} = -6 \times 10^{-3}\ T^{0.39}. \tag{3}$$

However, the large scattering of experimental results (the critical force values) does not allow us to assert that approximation (3) accurately describes the dependence $F_{\min}(T)$. Nevertheless, it demonstrates a steady tendency for the contact to increase its strength with the growth of its duration.

5. Conclusions

In this paper, we have described experiments on the indentation of steel indenters into the elastomer. The latter was a solidified aqueous solution of gelatin. It is found that, due to the corrosion, the contact between the indenter and the elastomer strengthened in time. Three different regimes depending on the contact duration are revealed. In the case of short-term contact, the indenter could be detached reversibly without damaging the elastomer surface. As the contact duration increased, the elastomer became partially destroyed, when the indenter was detached, and some quantity of the elastomer remained on the indenter surface. If the contact duration exceeded a certain critical value, the contact strengthened so much that, when the indenter was detached from the gelatin surface, the bulk destruction of gelatin took place. This occurred, because the chemical bonds between the indenter and the gelatin over the contact area became much stronger than the bonds between the gelatin molecules. In this case, a significant force has to be applied in order to detach the indenter, and this force turned out sufficient for the bulk destruction of the elastomer.

If the elastomer is partially destroyed, it is possible to carry out several cycles of indentation into its surface. In this case, all consecutive indentation cycles are characterized by different values of the normal force at which the contact collapses. The maximum force value is observed in the first cycle, when the contact is strengthened due to the corrosion processes. The subsequent indentation cycles demonstrate a reduction of the contact adhesive strength, because there are no more direct contacts between the indenter and the elastomer in some contact areas. Instead, we have a contact between the elastomer remaining on the indenter surface and the substrate elastomer itself, and such a contact has a much lower adhesive strength.

It is found that if the contact is rather long-lasting, the elastomer becomes thinner because of the moisture evaporation from its surface. As a result, the normal force decreases. This is a disadvantage of elastomers based on aqueous gelatin solutions, and it must be taken into account when processing experimental data.

The work was sponsored by the Deutsche Forschungsgemeinschaft (project PO 810-55-3).

1. H. Hertz. Über die Berührung fester elastischer Körper. *J. Reine Angew. Math.* **92**, 156 (1882).
2. J.N. Reddy. *An Introduction to the Finite Element Method (3rd Ed.)* (McGraw-Hill, 2005) [ISBN: 9780071267618].
3. P.K. Banerjee. *The Boundary Element Methods in Engineering (2nd Ed.)* (McGraw-Hill, 1994) [ISBN: 0-07-707769-5].
4. R. Pohrt, Q. Li. Complete boundary element formulation for normal and tangential contact problems. *Phys. Mesomech.* **17**, 334 (2014).
5. S.G. Psakhie, Y. Horie, S.Yu. Korostelev, A.Yu. Smolin, A.I. Dmitriev, E.V. Shilko, S.V. Alekseev. Method of movable cellular automata as a tool for simulation within the framework of mesomechanics. *Russ. Phys. J.* **38**, 1157 (1995).
6. M.H. Müser. Elastic contacts of randomly rough indenters with thin sheets, membranes under tension, half spaces, and beyond. *Tribol. Lett.* **69**, 25 (2021).
7. R. Pohrt, V.L. Popov. Adhesive contact simulation of elastic solids using local mesh-dependent detachment criterion in boundary elements method. *Facta Univ. Ser. Mech. Eng.* **13**, 3 (2015).
8. V.L. Popov, R. Pohrt, Q. Li. Strength of adhesive contacts: Influence of contact geometry and material gradients. *Friction* **5**, 308 (2017).
9. K.L. Johnson, K. Kendall, A.D. Roberts. Surface energy and the contact of elastic solids. *Proc. Roy. Soc. Lond. A* **324**, 301 (1971).
10. B.V. Derjaguin, V.M. Muller, Y.P. Toporov. Effect of contact deformations on the adhesion of particles. *J. Colloid Interf. Sci.* **53**, 314 (1975).
11. D. Maugis. Adhesion of spheres: the JKR-DMT-transition using a Dugdale model. *J. Colloid Interf. Sci.* **150**, 243 (1992).
12. M. Ciavarella, A. Papangelo. A generalized Johnson parameter for pull-off decay in the adhesion of rough surfaces. *Phys. Mesomech.* **21**, 67 (2018).
13. A. Pepelyshev, F.M. Borodich, B.A. Galanov, E.V. Gorb, S.N. Gorb. Adhesion of soft materials to rough surfaces: Experimental studies, statistical analysis and modelling. *Coatings* **8**, 350 (2018).
14. I.A. Lyashenko, R. Pohrt. Adhesion between rigid indenter and soft rubber layer: Influence of roughness. *Front. Mech. Eng.* **6**, 49 (2020).
15. V.L. Popov, Q. Li, I.A. Lyashenko, R. Pohrt. Adhesion and friction in hard and soft contacts: Theory and experiment. *Friction* **9**, 1688 (2021).
16. J.R. Parent, G.G. Adams. Adhesion-induced tangential driving force acting on a spherical particle lying on a sinusoidal surface. *J. Adhesion* **92**, 273 (2016).
17. I.A. Lyashenko, V.L. Popov, R. Pohrt, V. Borysiuk. High-precision tribometer for studies of adhesive contacts. *Sensors* **23**, 456 (2023).
18. I. Lyashenko, V. Borysiuk. Stick-slip motion in the contact between soft elastomer and spherical hard steel indenter: Model explanation of superplasticity mode in metal samples with grain boundary defects. *Procedia Struct. Integr.* **36**, 24 (2022).
19. V.L. Popov, M. Heß, E. Willert. *Handbook of Contact Mechanics. Exact Solutions of Axisymmetric Contact Problems* (Springer, 2019) [ISBN: 978-3-662-58708-9].
20. I.A. Lyashenko, V.L. Popov. Dissipation of mechanical energy in an oscillating adhesive contact between a hard indenter and an elastomer. *Tech. Phys. Lett.* **46**, 1092 (2020).
21. I. Argatov. Mechanics of heterogeneous adhesive contacts. *Int. J. Eng. Sci.* **190**, 103883 (2023).

Received 14.04.23.
Translated from Ukrainian by O.I. Voitenko

Я.О. Ляшенко, В.Л. Попов

ВПЛИВ КОРОЗІЙНИХ ПРОЦЕСІВ
НА АДГЕЗІЙНУ МІЦНІСТЬ КОНТАКТУ
МІЖ ЖОРСТКИМ ІНДЕНТОРОМ
І М'ЯКИМ ЕЛАСТОМЕРОМ: ЕКСПЕРИМЕНТ

Вивчається вплив тривалості контакту між сталевим індентором, який піддається корозії, і еластомером на основі водного розчину желатину, на адгезійну міцність контакту. Показано, що збільшення часу контакту приводить до його суттєвого зміцнення. У результаті контакт стає настільки міцним, що витягування індентора із еластомера призводить до руйнування поверхні еластомера.

Ключові слова: корозія, еластомер, адгезійна міцність, індентування, квазистатичний контакт.